Power C, Henry S, Del Bigio MR, Larsen PH, Corbett D, Imai Y, Yong VW, Peeling JIntracerebral hemorrhage induces macrophage activation and matrix metalloproteinases. Ann Neurol 53:...

Article *in* Annals of Neurology · June 2003

Impact Factor: 9.98 · DOI: 10.1002/ana.10553 · Source: PubMed

8 authors, including:

Marc R Del Bigio
University of Manitoba
239 PUBLICATIONS **7,164** CITATIONS
SEE PROFILE

Dale Corbett
University of Ottawa
155 PUBLICATIONS **7,256** CITATIONS
SEE PROFILE

Voon Wee Yong
The University of Calgary
305 PUBLICATIONS **16,896** CITATIONS
SEE PROFILE

Intracerebral Hemorrhage Induces Macrophage Activation and Matrix Metalloproteinases

Christopher Power, MD,[1] Scot Henry, BSc,[1] Marc R. Del Bigio, MD, PhD,[2] Peter H. Larsen, MSc,[1] Dale Corbett, PhD,[3] Yumi Imai, MD,[4] Voon Wee Yong, PhD,[1,5] and James Peeling, PhD,[6]

Intracerebral hemorrhage (ICH) is characterized by parenchymal hematoma formation with surrounding inflammation. Matrix metalloproteinases (MMPs) have been implicated in the pathogenesis of neurological diseases defined by inflammation and cell death. To investigate the expression profile and pathogenic aspects of MMPs in ICH, we examined MMP expression in vivo using a collagenase-induced rat model of ICH. ICH increased brain MMP-2, -3, -7, and -9 mRNA levels relative to sham-injected (control) animals in the vicinity of the hematoma, but MMP-12 (macrophage metalloelastase) was the most highly induced MMP (>80-fold). Immunohistochemistry showed MMP-12 to be localized in activated monocytoid cells surrounding the hematoma. In vitro studies showed that thrombin, released during ICH, induced MMP-12 expression in monocytoid cells, which was reduced by minocycline application. Similarly, in vivo minocycline treatment significantly reduced MMP-12 levels in brain. Neuropathological studies disclosed marked glial activation and apoptosis after ICH that was reduced by minocycline treatment. Neurobehavioral outcomes also were improved with minocycline treatment compared with untreated ICH controls. Thus, select MMPs exhibit increased expression after ICH, whereas minocycline is neuroprotective after ICH by suppressing monocytoid cell activation and downregulating MMP-12 expression.

Ann Neurol 2003;53:731–742

Intracerebral hemorrhage (ICH) represents 15 to 20% of all strokes as a primary event[1] and occurs with increasing frequency as a complication of thrombolytic treatment of ischemic stroke.[2] ICH is characterized by the induction of parenchymal inflammation within hours of ICH occurrence, initiated by adherence of leucocytes to damaged brain endothelia and subsequent brain entry.[3] The inflammatory molecules and their pathogenic effects on cell survival within the brain after ICH remain largely unknown, although we previously have shown that tumor necrosis factor (TNF)–α is upregulated in the brain after experimental ICH.[4,5] Other studies indicate that adhesion molecules[6] and glutamate levels[7] in brain are upregulated after ICH. Matrix metalloproteinases (MMPs) are a family of zinc-containing proteases that are involved in remodeling of the extracellular matrix, chemotaxis, and proteolytic cleavage of precursor molecules involved in cellular signaling.[8] MMPs have been implicated in several neurological diseases in which inflammation occurs, including multiple sclerosis, ischemic stroke, human immunodeficiency virus–associated dementia, and Alzheimer's disease (reviewed in Yong and colleagues[9]). Proinflammatory molecules including TNF-α and interleukin (IL)–1β regulate MMP expression, in part through NFκB transcriptional activity.[10] The most widely recognized pathogenic MMP effect is the disruption of cell–extracellular matrix contacts by MMPs, leading to apoptosis as a result of cell detachment and loss of integrin signaling.[11,12] Moreover, an interaction between MMPs and other molecules that regulate apoptosis also affects cell survival; an example is the MMP-7–mediated cleavage of Fas ligand.[13]

MMPs have been implicated in the pathogenesis of ischemic stroke in animal models and autopsy studies (reviewed in Mun-Bryce and Rosenberg[14]).[15–19] Studies of MMPS in ICH have focused on gelatin zymog-

From the [1]Department of Clinical Neurosciences, University of Calgary, Calgary, Alberta; [2]Department of Pathology, University of Manitoba, Winnipeg, Manitoba; [3]Department of Basic Medical Sciences, Memorial University, St. John's, Newfoundland, Canada; [4]Department of Neurochemistry, National Institute of Neuroscience, Tokyo, Japan. [5]Department of Oncology, University of Calgary, Calgary, Alberta; and [6]Department of Radiology, University of Manitoba, Winnipeg, Manitoba, Canada.

Received Aug 8, 2002, and in revised form Jan 16, 2003. Accepted for publication Jan 16, 2003.

Address correspondence to Dr Power, Neuroscience Research Group, Department of Clinical Neurosciences, HMRB 150, 3330 Hospital Dr. NW, University of Calgary, Calgary, Alberta, Canada T2N 4N1. E-mail: power@ucalgary.ca

raphy measurements of MMP-2 and -9.[20,21] Rosenberg and colleagues[20] and Lapchak and colleagues[21] reported that the intracerebral injection of a collagenase leads to ICH, edema, and necrosis, together with blood–brain barrier disruption. These effects are reduced by treatment with an endogenous inhibitor of MMPs, tissue inhibitor of metalloproteinase (TIMP)–2. Subsequently, the synthetic inhibitors of metalloproteinase activity, BB-1101 and BB-94, were shown to reduce edema and hemorrhage after bacterial collagenase or tissue plasminogen activator–induced ICH, respectively.[20,21]

The mechanisms remain incompletely understood by which MMPs and other proteases are pathogenic in neurological disease. Whether MMPs directly influence neuronal survival in ICH, or the mechanisms by which the MMP expression is regulated in ICH, remain unclear. Moreover, the temporal expression profiles of MMPs and TIMPs have not been described in ICH. Finally, whether inhibitors of MMP activity prevent neuronal and glial loss caused by ICH injury remains unknown. Herein, we investigate the profile of MMP expression after ICH and identify MMP-12 as a key molecule involved in mediating the outcome of ICH. We also report that a tetracycline derivative, minocycline, inhibits MMP-12 expression and provides neuroprotection from ICH injury.

Materials and Methods

Intracerebral Hemorrhage Model

Male Sprague-Dawley rats weighing 240 to 280gm were handled and cared for in accordance to the guidelines of the Canadian Council on Animal Care. Rats were anesthetized with pentobarbital (50mg/kg IP) and placed in a stereotaxic frame (David Kopf Instruments, Tujunga, CA). A 30-gauge needle was inserted through a burr hole into the striatum (location 3.5mm lateral to the midline, 0.2mm anterior to bregma, 6mm in depth below the skull). ICH was induced by administration of 0.5μl saline containing 0.05U of collagenase (type IV; Sigma, St. Louis, MO) over 5 minutes whereas sham-injected animals received 0.5μl of saline over the same duration.

Minocycline Treatment

Minocycline (Sigma) was given intraperitoneally at a dose of 45mg/kg 1 and 12 hours after ICH, followed by 22.5mg/kg twice daily until 1 week after ICH, and 22.5 mg/kg IP once daily for another week. These doses approximate those that have been used in experimental models of stroke[22] or multiple sclerosis.[23] Control rats received intraperitoneal injections of equivalent volumes of saline.

Cell Lines and Culture

U937 human monocytoid cells (ATCC, Rockville, MD) initially were cultured in RPMI-1640 containing 10% fetal calf serum, 100μg/ml streptomycin, and 0.25μg/ml amphotericin. Culture media was replaced with AIM V serum-free medium (GIBCO, Burlington, Ontario, Canada) for all experimental procedures because fetal calf serum contains various MMPs that would interfere with MMP zymographic analyses. To assess the effect of monocyte stimulation on IL-1β and MMP-12 expression, we treated cells with 50ng/ml of phorbol-12- myristate-13-acetate (PMA; Sigma; used as a positive control) for 18 hours or with 5IU of thrombin (Sigma) for 6 hours before harvest of supernatants and RNA isolation. Minocycline (Sigma) was applied to cultures at the time of stimulation and throughout the experiment at several concentrations.

Real-time Polymerase Chain Reaction

Groups of treated and control rats (n = 4 per group) were killed by cardiac perfusion with normal saline under pentobarbital anesthesia at 24 hours, 4, 7, 14, or 28 days after the induction of ICH, and brains were collected and analyzed for mRNA and protein levels. Brain tissue 2 to 4mm from the edge of the hematoma was dissected, homogenized, and then lysed in TRIzol (Life Technologies, Gaithersburg, MD) according to the manufacturer's guidelines. Total RNA was isolated and dissolved in diethylpyrocarbonate-treated water, 1μg RNA was used for the synthesis of complementary DNA, and polymerase chain reactions were performed as described previously. Primer sequences are displayed in the Table 1 Semiquantitative analysis was performed by monitoring in real time the increase of fluorescence of the SYBR-green dye on a Bio-Rad i-Cycler (Richmond, CA). Real-time fluorescence measurements were performed and a threshold cycle (C_τ) value for each gene of interest was calculated by determining the point at which the fluorescence exceeded a threshold limit (12-fold increase above the standard deviation of the initial baseline). To confirm single-band production, we performed melt-curve analysis and subsequently confirmed it by electrophoresis and ethidium bromide staining. All data were normalized against GAPDH mRNA level and expressed relative to sham-injected controls.

Zymography

MMP levels in conditioned media were measured by zymography as previously detailed,[24] except that casein (Bio-Rad 12% Zymogram Ready Gel with Casein) was used as a substrate for MMP-12. Sample volumes were normalized for the number of cells present in each culture at the time of harvest and concentrated 100-fold using Ultrafree-10 filters (Millipore, Bedford, MA) to facilitate detection of both the proenzyme and activated forms of MMP proteins. Gels were stained with 2.5mg/ml Brilliant Blue (Sigma) and destained in 40% methanol, 10% acetic acid. Stained gels were dried and MMP levels were determined by densitometry when in the linear range.

Western Blot

U937 cells (ATCC) cultured in Opti-MEM (Gibco) treated with PMA (50ng/ml) and/or minocycline (10μM) for 8 hours were homogenized in denaturation buffer (200mM Tris, pH 8.0, 4% SDS, 0.1% bromophenol blue, 40% glycerol, 5% β-mercaptoethanol). We used Bio-Rad Dc Protein Assay to quantify protein content, according to the manufacturer's instructions. Protein samples (20μg/lane) were sep-

Table. Primer Sequences Used in Polymerase Chain Reaction Amplification Including Size of the Amplicon and Optimal Annealing Temperature

Gene	Sequence	Length (bp)	Annealing Temperature (°C)
GAPDH	GCA TGG CCT TCC GTG TTC CTA CCC	110	58
GAPDHC	GGC CGC CTG CTT CAC CAC CTT CT		
MMP-2	TTG GTT TTG GCT GGC TTC TTC ACT	115	52
MMP-2 C	CGC ATT CTC GGT CAC AGG AT		
MMP-3	GAC CCC ACT CAC ATT CTC CA	109	52
MMP-3 C	GAC CAT TCC AGG CCC ATC AAA AG		
MMP-7	TGG CCT CAC TTT CAT TTT TGG TA	116	51
MMP-7 C	GGG CTG CAT TGG TCC TTA GTA		
MMP-9	TGT GGG GAG GGG TTT GGG GAG GAT A	195	80
MMP-9 C	TGA AAG GGA GGG AGG GGG ATG AAG C		
MMP-12	GGC GAG GCT GAC ATT ACG ATA CTT	112	53
MMP-12 C	GAA TAC CGG GCC CAG GAT AAA AA		
TIMP-1	CCT GGT TCC CTG GCA TAA TC	101	54
TIMP-1 C	TGG CTG AAC AGG GAA ACA CT		
TIMP-2	AGG GCC AAA GCA GTG AGC GAG AAG G	150	56
TIMP-2 C	TGA GGA GGG GGC CGT GTA GAT AAA T		
TIMP-3	ATC CGG CAG AAG GGT GGC TAC T	120	58
TIMP-3 C	GGG ATG GGA AGG AGG TGA GG		
TACE	AAG ACC CCA GCA CAG ATT CAC A	200	58
TACE C	AGG CCC AGG CTC CCA CTA ACA C		
IL-1β	GCA CCT TCT TTT CCT TCA TC	448	55
IL-1β C	CTG ATG TAC CAG TTG GGG AA		

arated in a 15% SDS-PAGE gel under reducing conditions and subsequently transferred to nitrocellulose membrane and probed with polyclonal anti–MMP-12 antibody (Chemicon, Temecula, CA; rabbit anti–MMP-12 N terminus [5μg/ml]). After incubation with horseradish peroxidase–conjugated secondary antibodies, antigens were visualized using BM Chemiluminesence Blotting Substrate (Boehringher-Mannheim, Mississauga, Ontario, Canada) according to the manufacturer's instructions.

Immunocytochemistry

Gliosis was assessed in serial sections (10μm) that were prepared as described previously[25] by immunostaining with antibodies to glial fibrillary acidic protein (GFAP; DAKO Diagnostics, Mississauga, ON) or the macrophage/microglial marker, Iba-1,[26] followed by two-step peroxidase anti-peroxidase staining. Double labeling was performed as previously reported,[27] with antibodies to GFAP (μg/ml) or Iba-1 (1μg/ml) and human MMP-12 (R & D Laboratories, Minneapolis, MN), using AP and DAB (Vector Laboratories, Burlingame, CA) with subsequent analysis of slides on a Zeiss Axioskop 2 upright microscope (Thornwood, NY).

Assessment of Acute Inflammation and Cell Death

At 1, 2, and 7 days after ICH, groups of four minocycline-treated and untreated rats were killed by cardiac perfusion with 4% paraformaldehyde under pentobarbital anesthesia, and the brains were removed. Brain sections (6μm) were stained with hematoxylin and eosin to assess neutrophils, racinus communis agglutinins (RCA)-1 lectin to label microglia and macrophages, and in situ DNA nick end labeling (TUNEL) to detect cells with damaged DNA (dying cells).[4,5] Using an ocular reticle and ×250 ocular magnification eosinophilic dying neurons, we counted TUNEL-positive dying cells, neutrophils, and RCA-1 binding cells in four fields (each area, 0.0625mm^2) immediately adjacent to the needle injection/damage site, which was defined by the presence of erythrocytes or necrosis. Areas with large blood vessels were avoided. The observer was blinded to the identity of the animal.

Magnetic Resonance Imaging

One day after ICH, magnetic resonance imaging (MRI) using a Bruker Biospec MSL-X 7/21 spectrometer was used to determine hematoma uniformity and to evaluate cerebral blood flow in the intact tissue around the hematoma for 10 minocycline-treated and 10 control rats. Coronal T_2-weighted images were acquired with a standard spin-echo sequence, executed using a 3.5 × 3.5cm^2 field of view, 1.0mm thick slice centered through the hematoma, 256 × 256 acquisition matrix, TR 1,650 milliseconds, TE 80 milliseconds, and 4 averages. Areas of the hematoma and of the cerebral hemispheres were measured directly from these images. Quantitative perfusion maps were obtained in the same location as the T_2-weighted images, using arterial spin tagging as preparation for TurboFLASH readout images. Labeling was performed with a radiofrequency (RF) field of 100mG and a 2G/cm gradient, with the RF offset (18,000Hz) chosen so that the labeling plane was located perpendicular to the long axis of the brain 5mm from the posterior edge of the cerebellum. The labeling time was 2.5 seconds, and a posttagging delay of 400 milliseconds was used to minimize vascular artifacts and the sensitivity to vari-

able transit time. A four-step protocol was used to control for the magnetization transfer effect. Perfusion images were calculated as described before, using λ (brain–blood partition coefficient) = 0.9, α (spin-tagging efficiency) = 0.75, and T_1 = 1.7 seconds. The hematoma was mapped on the T_2-weighted image for each rat, along with regions of interest (ROIs) adjacent to and slightly removed from the hematoma. Control ROIs were defined for identical locations in the contralateral hemisphere. These ROIs then were superimposed on the corresponding perfusion image, and the cerebral blood flow in each ROI around the hematoma was determined relative to that in the corresponding ROI on the contralateral side. Perfusion MRIs also were obtained from rats without ICH but treated with minocycline or vehicle as described above.

Neurobehavioral Evaluation

The rats examined by MRI were weighed daily. Neurobehavioral deficits were evaluated by an observer blinded to the treatment identity at 1, 2, 7, 14, 21, and 28 days after ICH induction. The tests used were as previously described.[4] In brief, they included (1) spontaneous ipsilateral circling behavior, graded from 0 for no circling to 4 for continuous; (2) contralateral forelimb flexion, graded from 0 for uniform extension of both forelimbs to 2 for full wrist flexion and shoulder adduction; and (3) ability to walk a 70cm long × 2.4cm wide wood beam, graded from 0 for normal movement along the beam to 4 for no movement or for a rat that fell off the beam. The behavioral score was reported as a cumulative score of the three tests with a maximum total score of 10.

Effect of Minocycline on Temperature after Intracerebral Hemorrhage

To determine whether minocycline has a direct effect on body temperature in ICH, we implanted temperature probes (XMFH probes; MiniMiter, Bend, OR) under halothane anesthesia into the peritoneal cavity of 11 rats. Beginning 2 to 5 days later, ICH was induced in each rat and treatment was initiated as described above (minocycline, n=6; control, n=5). Core temperature was sampled automatically every 30 seconds and averaged into 10-minute blocks for 48 to 54 hours after ICH induction.[28]

Statistical Analysis

Statistical analyses were performed using Instat, version 3.0 (Graphpad Software) for both parametric and nonparametric comparisons. p values of less than 0.05 were considered significant. Data were analyzed to ensure normal distribution and intergroup comparisons were made by analysis of variance followed by Bonferroni or Dunn post hoc tests.

Results

In Vivo Matrix Metalloproteinase Profile after Intracerebral Hemorrhage

Earlier studies[20,21,29] showed that MMP-2 and -9 are increased after ICH, although the temporal profile of expression of MMPs was not examined. To define the expression of MMPs over time after ICH induction, we prepared striatal tissue adjacent to the site of the ICH for real-time reverse transcription polymerase chain reaction analysis from sham-injected (control) animals and ICH animals at 1, 4, 7, 14, and 28 days after ICH induction. Analysis of the mean relative fold increase (RFI ± standard error of the mean) in mRNA abundance showed that MMP-2 expression was significantly increased at day 7 (3.6 ± 0.37 RFI) after induction of ICH (Fig 1A), whereas MMP-3 levels were increased (3.4 ± 0.69 RFI) at 24 hours after ICH (see Fig 1B). Similarly, MMP-7 was also significantly increased above baseline at 24 hours (12.6 ± 0.89 RFI) and at day 7 (4.6 ± 0.77 RFI) after ICH (see Fig 1C). MMP-9 displayed significantly elevated mRNA levels relative to controls at 24 hours (3.9 ± 0.42 RFI) and 7 days (4.3 ± 0.77 RFI; see Fig 1D). However, the most highly induced MMP in this study was MMP-12, which was markedly enhanced at day 7 (86.8 ± 11.24 RFI) after ICH, although not at other time points (see Fig 1E).

Examination of tissue inhibitors of metalloproteinases (TIMPs) showed that TIMP-1 was increased at 7 days relative to controls, whereas TIMP-2 was reduced at 24 hours and 7 days after ICH (see Fig 1F, G, respectively). Similarly, TIMP-3 also exhibited significantly reduced levels relative to control animals at day 7 (see Fig 1H). These findings suggested that several MMPs, including MMP-2, -7, and particularly MMP-12, exhibited marked increases in abundance after ICH.

Cells of monocytoid lineage express MMP-12,[30] although its detection also has been reported in cerebral endothelial cells under inflammatory conditions[31] as well as in brain tumors.[32] To determine which cells expressed MMP-12 after ICH, we performed immunohistochemical studies using sections from animals with ICH. These showed that MMP-12 expression was detectable near the ICH lesion (Fig 2). The MMP-12–immunopositive cells were round, amoeboid-appearing cells, resembling activated macrophages, and were chiefly localized in the parenchymal margin immediately around the site of hemorrhage (see Fig 2A). Double-label immunostaining with antibodies to Iba-1 or GFAP showed colocalization of MMP-12 with Iba-1 but not GFAP (see Fig 2B). Thus, the principal source of MMP-12 after ICH was activated macrophages and microglia.

In Vitro Effects of Minocycline

Because minocycline has been shown to influence the extent of inflammation including MMP expression,[23] we analyzed the expression in monocytoid cells of MMP-12 and IL-1β, which is known to stimulate MMP-12 production.[33] U937 cells were stimulated with PMA at several concentrations, which showed that treatment with 50ng/ml of PMA was the most

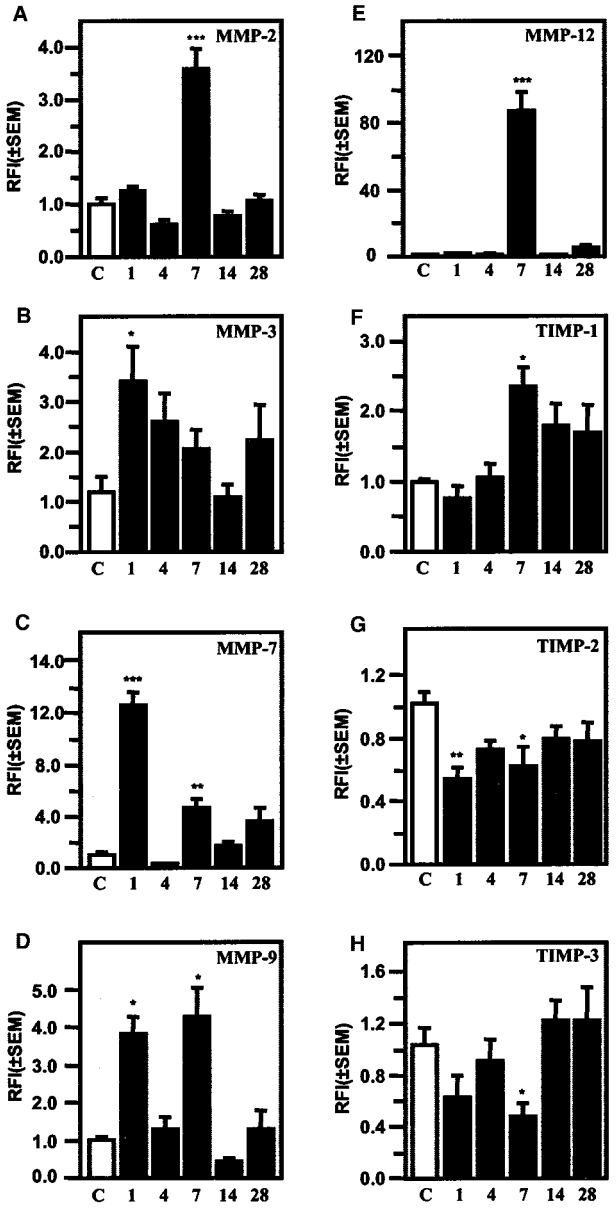

*Fig 1. Matrix metalloproteinase (MMP) RNA levels after intracerebral hemorrhage (ICH), expressed as relative fold increases (RFIs). (A) MMP-2 levels were selectively increased at 7 days after ICH compared with sham-implanted (control) animals. (B) MMP-3 levels were increased at 24 hours after ICH but reduced at subsequent time points. (C) MMP-7 levels were increased initially after ICH at 24 hours and also at 7 days. (D) MMP-9 levels were increased at 24 hours and 7 days after ICH relative to sham-inoculated animals. (E) MMP-12 levels were selectively increased at day 7 after ICH, exhibiting the greatest relative fold increase of all the studied MMPs after ICH. (F) TIMP-1 mRNA levels were increased at day 7 after ICH. (G) TIMP-2 levels were selectively reduced at days 1 and 7 after ICH compared with sham. (H) TIMP-3 levels were reduced relative to sham-inoculated animals at days 1 and 7 after ICH (*single asterisks, $p < 0.05$; double asterisks, $p < 0.01$; triple asterisks, $p < 0.001$). *SEM = standard error of the mean.*

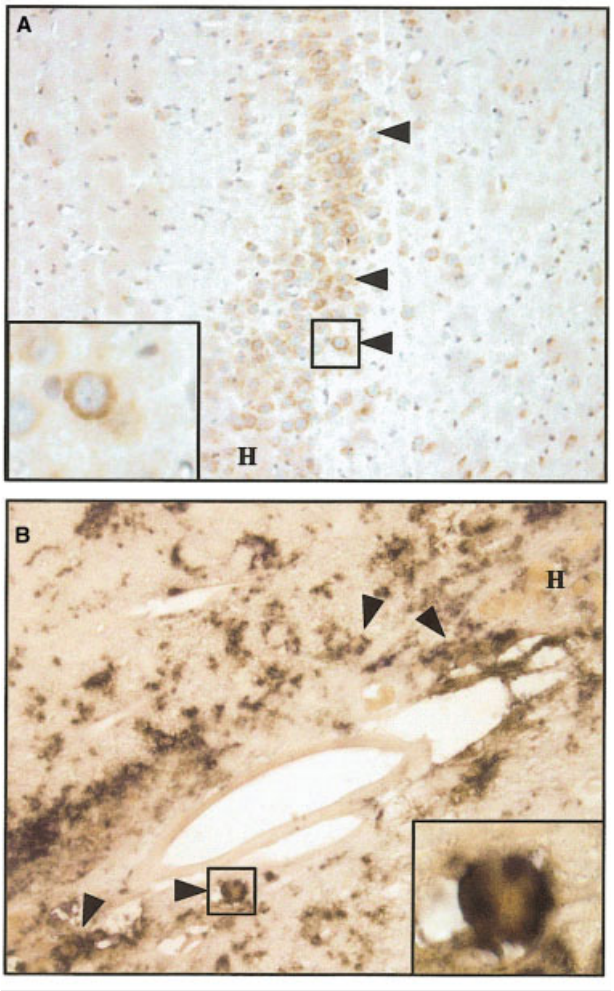

Fig 2. Immunodetection of MMP-12 after intracerebral hemorrhage (ICH). (A) MMP-12 (brown immunoreactivity; arrowheads*) was detected in perilesional monocytoid cells* (inset) *with peak expression at day 7 after ICH. (B) To confirm that MMP-12 was being produced by cells of monocyte lineage, we conducted double labeling with antibodies to Iba-1* (blue) *and MMP-12* (brown) *that showed that Iba-1–immunopositive macrophages also expressed MMP-12 (H-hematoma) (original magnification ×200).*

potent stimulus of IL-1β (Fig 3A) and MMP-12 (see Fig 3B). U937 cells were treated with minocycline at two concentrations and at the time of PMA stimulation. These experiments showed that IL-1β mRNA expression was significantly reduced with the treatment of minocycline (see Fig 3A). MMP-12 mRNA levels also were reduced, although this was not statistically significant (see Fig 3B).

Because thrombin is released into the brain during ICH, we treated U937 cells with thrombin, which showed that thrombin (5IU) potently induced MMP-12 mRNA expression (see Fig 3C), although IL-1β was unaffected by thrombin (data not shown). Induction of MMP-12 by thrombin also was signifi-

cantly reduced by concurrent minocycline treatment, indicating that minocycline regulated the in vitro expression of MMP-12. Subsequent Western blotting showed that MMP-12 protein levels were markedly reduced in cultures treated with minocycline (see Fig 3D) after thrombin activation; this was evident for all three forms of MMP-12 (proform of 54kDa, intermediate form of 45kDa, and active form of 22kDa). To confirm these Western blot results, we performed zymography on concentrated supernatants from treated U937 cells, which showed that active MMP-12 protein expression was reduced by minocycline (see Fig 3E). These in vitro findings suggested that MMP-12 was induced in monocytoid cells and the induction was reduced by minocyline treatment.

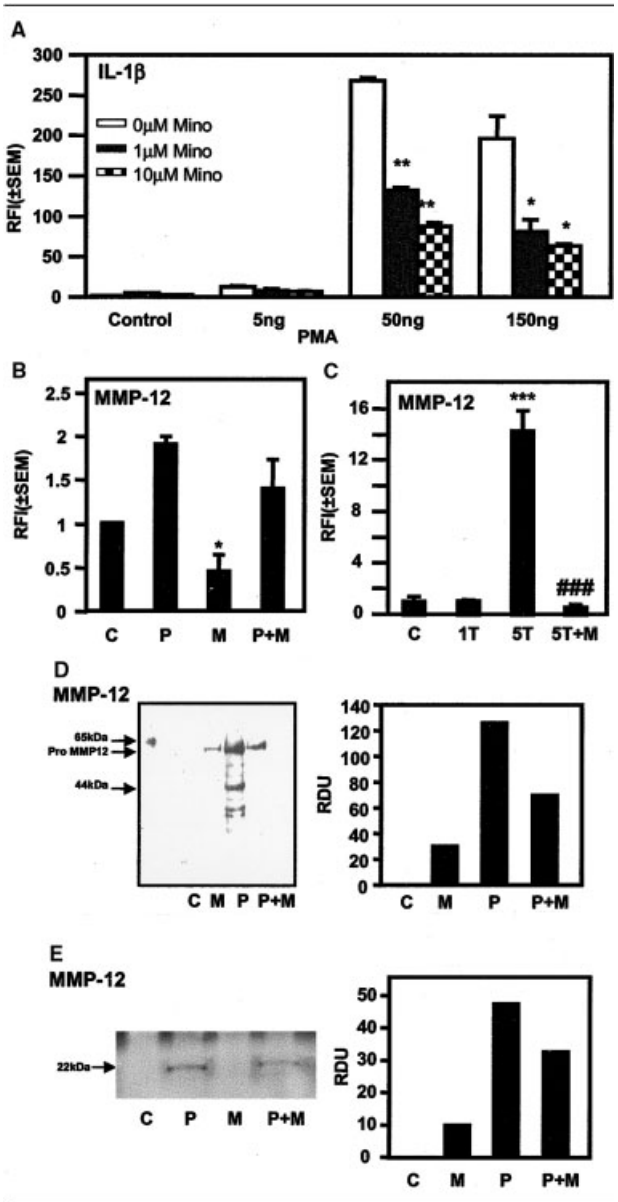

*Fig 3. In vitro detection of interleukin (IL)–1β and MMP-12 mRNA and protein. (A) PMA (50ng/ml) was found to optimally stimulate IL-1β in U937 monocytoid cells. In addition, minocycline was found to inhibit IL-1β expression maximally in vitro at 10μM. (B) Similarly, PMA (P) was found to induce MMP-12 expression in monocytoid cells with a trend towards a reduction (nonsignificant) after minocycline (M) treatment (1μM). (C) Thrombin (T, at 5IU) was found to be a potent inducer of MMP-12 expression in monocytoid cells, and this induction was inhibited by concurrent treatment by minocycline (1μM). (D) MMP-12 protein production (proform of 54kDa, intermediate form of 45kDa, and active form of 22kDa) was increased with PMA stimulation and subsequently inhibited with minocycline treatment (1μM) as shown by Western blotting. The relative density for pro–MMP-12 is shown in the right-hand panel, whereas active MMP-12 was detectable only with the PMA stimulation alone. (E) Like immunoblotting, casein zymography also showed increased MMP-12 activity with PMA treatment, which subsequently was reduced with minocycline. The corresponding relative density unit (RDU) plots are shown for Western blot and zymographic detection of MMP-12 abundance and activity, respectively, in the right-hand panel (*single asterisks, $p < 0.05$; double asterisks, $p < 0.01$; triple asterisks, $p < 0.001$). RFI = relative fold increase.*

Neuropathological Studies of Minocyline Effects on Intracerebral Hemorrhage

Since MMP-12 was markedly enhanced after ICH and minocycline appeared to be a potent regulator of MMP-12 expression, animals in which ICH was induced were also treated with minocycline. We examined the effects of minocycline on glial activation by immunostaining of microglia/macrophages and astrocytes. These studies disclosed that Iba-1–immunopositive cells occasionally were identified in sham-injected (control) animals (Fig 4). However, markedly increased expression of Iba-1 was apparent on infiltrating macrophages and parenchymal microglia in ICH animals at days 4 (see Fig 4B) and 7 (see Fig 4C) after ICH, complemented by increased GFAP immunoreactivity on astrocytes in the vicinity of the hematoma (*H*). For both glial-directed antibodies, cell body hypertrophy accompanied the increase in protein detection in ICH-untreated animals. By day 28, microglial immunoreactivity was limited to the immediate margin of the hematoma (data not shown). Minocycline treatment reduced Iba-1 immunostaining on both microglia and macrophages at days 3 (see Fig 4D) and 7 (see Fig 4E), suggesting that minocycline reduced glial activation after ICH.

Early events occurring after acute neurovascular injuries can affect long-term outcome,[1] and thus we examined the early neuropathological features in minocycline-treated and untreated animals by quantifying neutrophil infiltration, TUNEL detection of cell death, and the presence of activated macrophages and

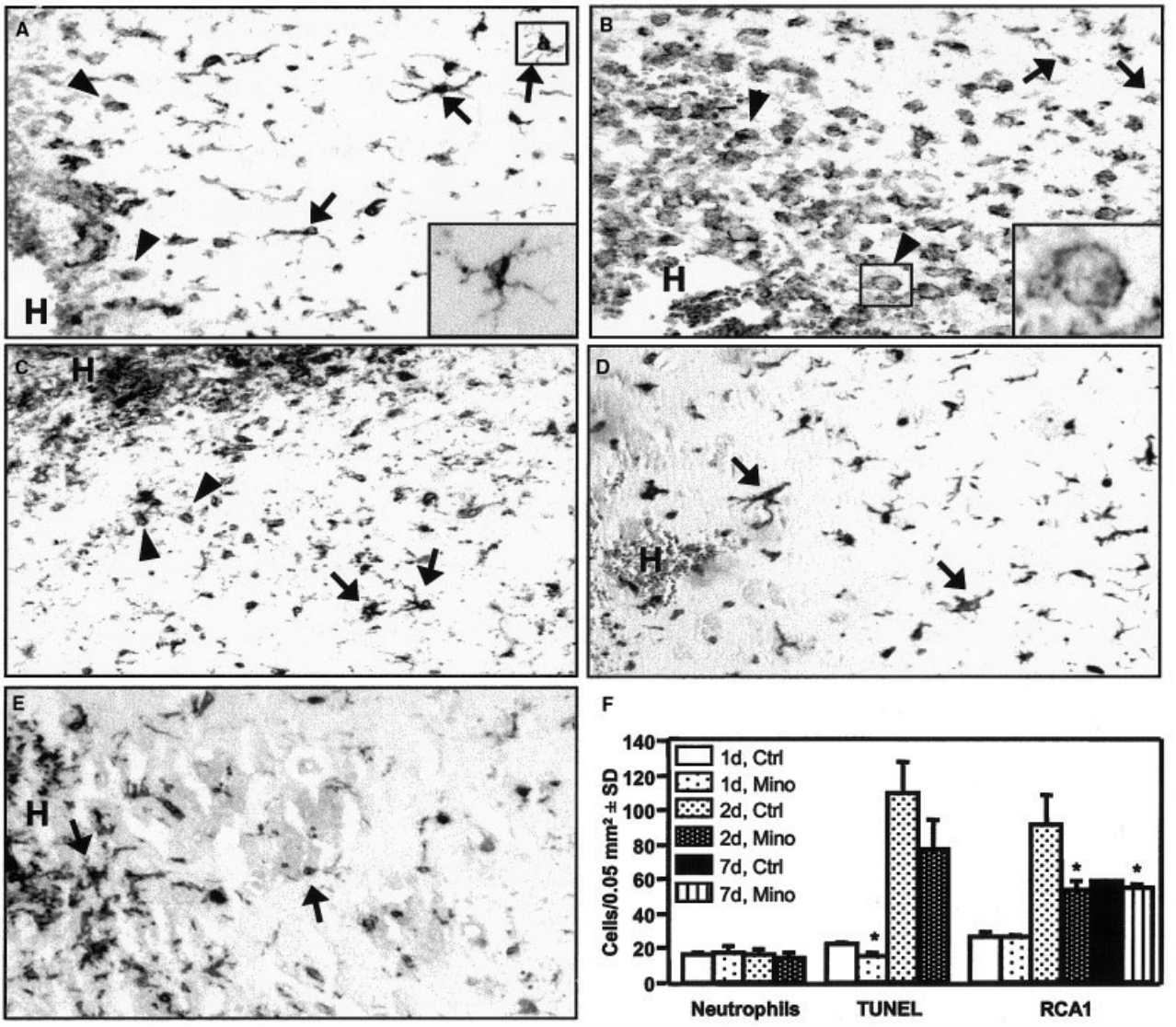

Fig 4. Immunopathological changes after intracerebral hemorrhage (ICH). (A) Microglia were detectable in sham-injected animals. At 3 (B) and 7 (C) days after ICH, microglia/macrophage immunoreactivity for Iba-1 was markedly increased in the vicinity of the hematoma (**H**); hypertrophied microglial cells (arrows) *and ameboid macrophages* (arrowheads) *were evident. Minocycline treatment reduced macrophage infiltration and microglia hypertrophy after ICH at 3 (D) and 7 (E) days. (F) Neuropathological changes after ICH and the effects of minocycline. Neutrophil infiltration after ICH (Ctrl) was not influenced by coincident minocycline treatment (Mino). In contrast, TUNEL detection of cell death was reduced at day 1 with a trend toward reduction at day 2 after ICH with minocycline treatment. Similarly, macrophage infiltration as indicated by RCA detection was selectively reduced at days 2 and 7 after ICH (*asterisk, $p < 0.05$; *original magnification, ×200).*

microglia in the immediate vicinity of the hematoma (see Fig 4F). Treatment with minocycline did not affect neutrophil levels but the number of TUNEL-positive cells at day 1 after ICH was reduced by minocycline (see Fig 4F). Furthermore, RCA detection for macrophage/microglia showed significantly reduced numbers in minocycline-treated animals at days 2 and 7. From these studies, we concluded that minocycline reduced cell death and the activation of microglia and/or macrophages around the area of injury after ICH.

In Vivo Effects of Minocycline on mRNA Levels

To investigate the in vivo effects of minocycline on MMP mRNA levels, we compared mRNA levels after ICH with and without concurrent minocycline treatment. These studies showed that minocycline did not have any effects on MMP-2 (Fig 5A), MMP-7 (see Fig

5B), or MMP-9 (see Fig 5C) mRNA levels. Similarly, minocycline had no effect on TIMP-1, -2, and -3 mRNA abundance (data not shown). However, MMP-12 expression was significantly reduced at day 7 after ICH induction (see Fig 5D), the time point at which it was most highly activated. This finding was complemented by similar findings, suggesting that IL-1β expression also was reduced by minocycline treatment at all time points (see Fig 5E), although this achieved statistical significance only at days 14 and 28 after ICH. These mRNA-related observations were supported by the lack of MMP-12 protein detection by immunocytochemistry at day 7 in minocycline-treated animals (data not shown). Collectively, the above findings suggested that minocycline may act by regulating MMP-12 expression in vivo, similar to the in vitro observations.

Effect of Minocycline on Magnetic Resonance Imaging, Temperature, and Behavioral Outcomes after Intracerebral Hemorrhage

T2-weighted MRIs showed that ICH lesion size was similar for untreated (Fig 6A) and minocycline-treated (see Fig 6B) animals. Similarly, MR perfusion images showed no changes in striatal or cortical blood flow after minocycline administration for up to 7 days in rats without ICH. After ICH, blood flow in the tissue immediately around the hematoma was decreased, with no difference between rats treated with minocycline or vehicle (data not shown). In the 4-hour period immediately after ICH, body temperature decreased to 36.5 ± 0.5°C in rats treated with minocycline and to 36.4 ± 0.4°C in vehicle-treated animals. Subsequent measurements showed that body temperature returned to normal and remained unchanged out to 48 hours after ICH (minocycline group, 37.7 ± 0.5°C; control group, 37.7 ± 0.4°C). However, neurobehavioral abnormalities caused by ICH were abrogated by treatment with minocycline with a trend beginning at day 1 (see Fig 6C), but reaching statistical significance by day 7, which persisted until day 28 after ICH.

Discussion

In this study, we found several MMPs to be selectively increased after ICH. Like earlier reports,[20] both MMP-2 and -9 were increased in the brains of animals with ICH. However, MMP-12 was most strikingly elevated at day 7 after ICH, largely in perilesional macrophages. Similarly, MMP-12 was induced in cultured monocytoid cells after PMA and thrombin stimulation. Of therapeutic importance, minocycline selectively diminished MMP-12 mRNA and protein abundance in both in vitro and in vivo assays. These latter observations were accompanied by improved quantitative neuropathological and neurobe-

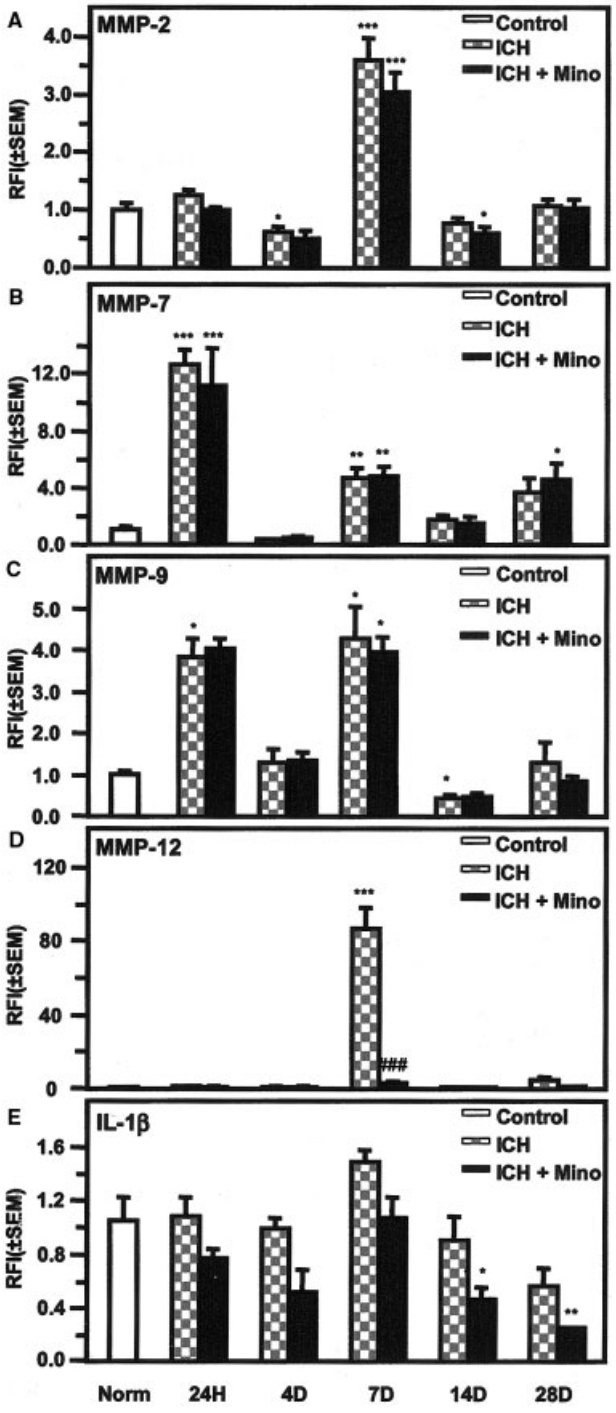

*Fig 5. Minocycline inhibits MMP-12 expression in vivo after intracerebral hemorrhage (ICH). Although MMP-2 (A), MMP-7 (B), and MMP-9 (C) mRNA expression levels were not influenced by minocycline treatment, MMP-12 (D) and interleukin (IL)–1β (E) expression was significantly reduced in the vicinity of the ICH lesion by concurrent treatment with minocycline (*single asterisks, $p < 0.05$; double asterisks, $p < 0.01$; triple asterisks, $p < 0.001$). *RFI = relative fold increase; SEM = standard error of the mean.*

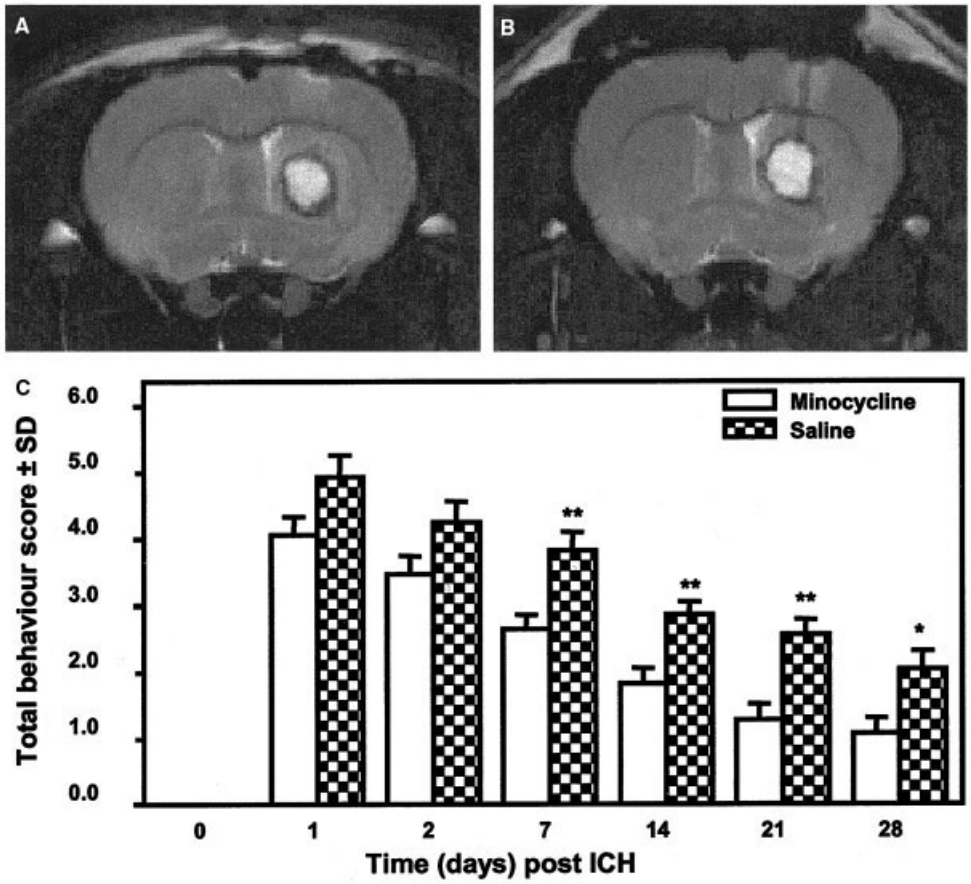

*Fig 6. Neuroimaging and neurobehavioral abnormalities after intracerebral hemorrhage (ICH). Untreated (A) and minocycline-treated (B) ICH animals did not differ in the size of the T2-weighted lesion at day 1 after ICH induction. In contrast, minocycline treatment improved neurobehavioral performance (C) after ICH with a trend beginning at day 1 but reaching statistical significance at day 7, which was maintained until day 28 after ICH (*single asterisk, $p < 0.05$; double asterisk, $p < 0.01$). *SD = standard deviation.*

havioral features, indicating that reduced expression of a specific MMP by minocycline improved neurological outcome.

ICH represents a major subset of strokes including primary ICH resulting from hypertension, vascular anomalies, bleeding diatheses, and secondary hemorrhagic transformation of ischemic infarcts.[1] The immediate mechanisms by which cellular injury occurs during ICH include mechanical compression of tissue due to blood accumulation and edema, impairment of local blood flow, and extravasation into the brain parenchyma of blood that contains potentially damaging molecules such as thrombin and plasmin.[3,4] Inflammatory cells are activated within hours of ICH initiation, initiated by adherence of neutrophils to damaged brain endothelia and subsequent brain entry.[3] Macrophages follow neutrophils into the brain within hours to days after ICH occurrence, and there is activation of resident microglia and astrocytes, accompanied by neuronal and glial cell death. Given the importance of MMPs during inflammation within the brain,[9] it would be anticipated that MMP expression was induced by ICH. Several MMPs (-3, -7, and -9) were increased immediately after ICH with subsequent reduction in mRNA levels at day 3 after ICH. However, there was a second increase in MMP-7 and -9 at day 7 after ICH followed by a reduction in mRNA levels. This biphasic increase in MMP expression may reflect cellular infiltration and subsequent activation including early neutrophil entry followed by monocyte/macrophage infiltration and activation in response to extravasated blood within the brain. TIMP expression after ICH varied depending on the individual molecule with TIMP-1 increased after ICH, whereas TIMP-2 and -3 were reduced after ICH. Of relevance, TIMP-2 and -3 are potent, and constitutively expressed, inhibitors of several MMPs, and, hence, their reduction may enhance the actions of MMPs within the brain.[9,29] Although we previously have shown that TNF-α expression is increased in this model of ICH,[4] we did not

find consistent changes in TACE mRNA after ICH (data not shown), which was surprising because of its significance in the neuropathogenesis of other diseases. Although these observations support a role for MMPs in the pathogenesis of ICH, the currently studied MMPs represent only a subset of metalloproteinases found within the brain, and future studies will require examination of related proteases to fully define their expression profile after ICH.

Despite ICH being a frequent type of stroke, there are few models that recapitulate its clinical and neuropathological features. Nonetheless, our model reflects many of the key aspects of ICH including neurobehavioral, neuroimaging, and neuropathological features. However, one fundamental difference is that the blood vessels are disrupted in this model by the injection of bacterial collagenase. Although this can be viewed as a potential criticism of the model, studies done by our group indicate that there was no difference observed in the MMP mRNA profile between collagenase-injected animals and animals injected with autologous blood (data not shown), another model of ICH injury. In both ICH models, cell death involving neurons and glia is a cardinal feature of tissue injury. Moreover, inflammation is a common feature to both models of ICH with initial neutrophil infiltration followed by monocytoid infiltration and activation within the brain.[3] Accompanying the cellular changes in ICH is the upregulation of several families of proinflammatory genes including MMPs.[4,5] Earlier studies by Rosenberg and colleagues using gelatin zymography showed that MMP-2 and -9 are upregulated after ICH,[20] and our results extend these observations by showing that increased transcription of several MMPs occurs after ICH. The significance of these findings is considerable given that MMP-2 is thought to be neurotoxic as shown in models of human immunodeficiency virus infection.[35] MMPs can promote inflammation as illustrated by the ability of both TACE and MMP-7 to cleave pro–TNF-α, resulting in its enhanced activity. Nevertheless, we found that MMP-12 expression was especially induced by ICH injury. MMP-12 is also induced, along with other MMPs, in a model of multiple sclerosis in rats.[36] Although we did not quantify MMP-12 protein expression or activity in vivo because of the difficulty performing casein zymography or MMP-12 immunoblotting in brain tissue, the increased immunoreactivity of MMP-12 on brain sections from ICH animals together with the close coupling of MMP-12 mRNA and protein expression indicates that reduction of MMP-12 expression with minocycline is both an in vitro and in vivo phenomenon. Moreover, the activation of monocytoid cells was accompanied by increased MMP-12 expression and release by these cells. The substrates for MMP-12 (metalloelastase) include casein, elastin, fibronectin, laminin, proteoglycon link protein, and vitronectin.[9] However, proteolysis of these molecules has not been associated with cell death, with the exception of the degradation of laminin, ultimately leading to neuronal death.[12] Hence, an important question regarding the potential substrates for MMP-12 that mediates cellular damage after ICH remains to be answered.

Earlier studies indicate that minocycline is neuroprotective after cerebral ischemia, demyelination, and neurotrauma.[22,37,38] Minocycline's mechanism of action remains unclear, although studies suggest that it may downregulate microglia activation,[39] caspase activity,[40] and other select signaling pathways.[41] Minocycline recently was found to inhibit the release of cytochrome *c* from mitochondria, which is key step in the induction of apoptosis.[42] These latter findings complement our results in which we show diminished in vivo cell death with minocycline treatment after ICH. Hypothermia has been shown consistently to be neuroprotective (reviewed in Corbett and Nurse[43]), but in our studies we found that minocycline did not induce hypothermia when animals were treated for several weeks. Similarly, perfusion imaging did not show a difference in blood flow around the lesion between minocycline-treated and untreated animals, indicating that its neuroprotective effects were independent of blood flow in these studies. In both minocycline-treated and untreated animals, there was a decline in body weight after ICH induction, but animals in the minocycline group did not gain weight subsequently at the same rate as those in the untreated group (data not shown). However, in long-term human use for the treatment of acne, the toxicity of minocycline has been unremarkable and weight loss has not been reported.[44–47]

In summary, minocycline selectively reduced MMP-12 mRNA and protein abundance and activity but did not affect other MMP levels, suggesting that minocycline's actions are comparatively specific in this model of ICH injury. In addition, minocycline reduced macrophage activation, similar to previous studies showing a downregulation of microglia during Experimental Allergic Encephalomyelitis (EAE),[38] ischemic injury,[38] and in an animal model of Parkinson's disease.[48] These, and other mechanisms described above, highlight the neuroprotective effects of minocycline in a variety of central nervous system injuries. There are few therapies for ICH, and with its established safety profile in humans, minocycline is an appealing therapeutic option for ICH. Moreover, the recent implication of MMPs in hemorrhagic transformation of ischemic stroke after thrombolytic therapy underscore the importance of MMPs in the pathogenesis of stroke.[49–51] Further studies focused on the precise mechanism of its inhibition of MMP-12,

and potential substrates for MMP-12 are required to further elucidate the pathogenic mechanisms after ICH.

These studies were supported by CIHR, the Heart and Stroke Foundation of Canada, and the Canadian Stroke Network (NCE).

C.P. is an AHFMR Scholar/CIHR Investigator and V.W.Y. is an AHFMR Senior Scholar/CIHR Scientist.

We thank B. Ibrahim for assistance with manuscript preparation, and J. Ethier, M. Xue, and H. J. Yan for technical assistance.

References

1. Qureshi AI, Tuhrim S, Broderick JP, et al. Spontaneous intracerebral hemorrhage. N Engl J Med 2001;344:1450–1460.
2. Lapchak PA. Hemorrhagic transformation following ischemic stroke: significance, causes, and relationship to therapy and treatment. Curr Neurol Neurosci Rep 2002;2:38–43.
3. Del Bigio MR, Yan HJ, Buist R, et al. Experimental intracerebral hemorrhage in rats. Magnetic resonance imaging and histopathological correlates. Stroke 1996;27:2312–2319.
4. Mayne M, Ni W, Yan HJ, et al. Antisense oligodeoxynucleoide inhibition of tumor necrosis factor is neuroprotective following intracerebral hemorrhage. Stroke 2001;32:240–248.
5. Mayne M, Fotheringham J, Yan HJ, et al. Adenosine A2A receptor activation reduces proinflammatory events and decreases cell death following intracerebral hemorrhage. Ann Neurol 2001;49:727–735.
6. Gong C, Hoff JT, Keep RF. Acute inflammatory reaction following experimental intracerebral hemorrhage in rat. Brain Res 2000;871:57–65.
7. Castillo J, Davalos A, Alvarez-Sabin J, et al. Molecular signatures of brain injury after intracerebral hemorrhage. Neurology 2002;58:624–629.
8. Galis ZS, Khatri JJ. Matrix metalloproteinases in vascular remodeling and atherogenesis: the good, the bad, and the ugly. Circ Res 2002;90:251–262.
9. Yong VW, Power C, Forsyth P, Edwards D. Metalloproteinases in the biology and pathology of the nervous system. Nat Neurosci 2001;2:502–511.
10. Lee WH, Kim SH, Lee Y, et al. Tumor necrosis factor receptor superfamily 14 is involved in atherogenesis by inducing proinflammatory cytokines and matrix metalloproteinases. Arterioscler Thromb Vasc Biol 2001;21:2004–2010.
11. Ruoslahti E, Reed JC. Anchorage dependence, integrins, and apoptosis. Cell 1994;77:477–478.
12. Chen ZL, Strickland S. Neuronal death in the hippocampus is promoted by plasmin-catalyzed degradation of laminin. Cell 1997;91:917–925.
13. Powell WC, Fingleton B, Wilson CL, et al. The metalloproteinase matrilysin proteolytically generates active soluble Fas ligand and potentiates epithelial cell apoptosis. Curr Biol 1999; 9:1441–1447.
14. Mun-Bryce S, Rosenberg GA. Matrix metalloproteinases in cerebrovascular disease. J Cereb Blood Flow Metab 1998;18: 1163–1172.
15. Clark AW, Krekoski CA, Bou SS, et al. Increased gelatinase A (MMP-2) and gelatinase B (MMP-9) activities in human brain after focal ischemia. Neurosci Lett 1997;238:53–56.
16. Romanic AM, White RF, Arleth AJ, et al. Matrix metalloproteinase expression increases after cerebral focal ischemia in rats: inhibition of matrix metalloproteinase-9 reduces infarct size. Stroke 1998;29:1020–1030.
17. Heo JH, Lucero J, Abumiya T, et al. Matrix metalloproteinases increase very early during experimental focal cerebral ischemia. J Cereb Blood Flow Metab 1999;19:624–633.
18. Gasche Y, Copin JC, Sugawara T, et al. Matrix metalloproteinase inhibition prevents oxidative stress-associated blood-brain barrier disruption after transient focal cerebral ischemia. J Cereb Blood Flow Metab 2001;21:1393–1400.
19. Fujimura M, Gasche Y, Morita-Fujimura Y, et al. Early appearance of activated matrix metalloproteinase-9 and blood-brain barrier disruption in mice after focal cerebral ischemia and reperfusion. Brain Res 1999;842:92–100.
20. Rosenberg GA, Navratil M. Metalloproteinase inhibition blocks edema in intracerebral hemorrhage in the rat. Neurology 1997; 48:921–926.
21. Lapchak PA, Chapman DF, Zivin JA. Metalloproteinase inhibition reduces thrombolytic (tissue plasminogen activator)-induced hemorrhage after thromboembolic stroke. Stroke 2000; 31:3034–3040.
22. Yrjanheikki J, Keinanen R, Pellikka M, et al. Tetracyclines inhibit microglial activation and are neuroprotective in global brain ischemia. Proc Natl Acad Sci USA 1998;95: 15769–15774.
23. Brundula V, Rewcastle NB, Metz L, et al. Targeting leukocyte MMPs and transmigration: minocycline as a novel therapeutic for multiple sclerosis. Brain 2002;125:1297–1308.
24. Oh LY, Larsen PH, Krekoski CA, et al. Matrix metalloproteinase-9/gelatinase B is required for process outgrowth by oligodendrocytes. J Neurosci 1999;19:8464–8475.
25. Power C, Kong PA, Crawford TO, et al. Cerebral white matter changes in acquired immunodeficiency syndrome dementia: alterations of the blood-brain barrier. Ann Neurol 1993;34: 339–350.
26. Imai Y, Ibata I, Ito D, et al. A novel gene iba1 in the major histocompatibility complex class III region encoding an EF hand protein expressed in a monocytic lineage. Biochem Biophys Res Commun 1996;224:855–862.
27. Johnston JB, Silva C, Gonzalez G, et al. Diminished adenosine A1 receptor expression on macrophages in brain and blood of patients with multiple sclerosis. Ann Neurol 2001; 49:650–658.
28. Colbourne F, Corbett D. Delayed postischemic hypothermia: a six month survival study using behavioral and histological assessments of neuroprotection. J Neurosci 1995;15: 7250–7260.
29. Rosenberg GA, Kornfeld M, Estrada E, et al. TIMP-2 reduces proteolytic opening of blood-brain barrier by type IV collagenase. Brain Res 1992;576:203–207.
30. Wu L, Fan J, Matsumoto S, Watanabe T. Induction and regulation of matrix metalloproteinase-12 by cytokines and CD40 signaling in monocyte/macrophages. Biochem Biophys Res Commun 2000;269:808–815.
31. Hummel V, Kallmann BA, Wagner S, et al. Production of MMPs in human cerebral endothelial cells and their role in shedding adhesion molecules. J Neuropathol Exp Neurol 2001; 60:320–327.
32. Beliveau R, Delbecchi L, Beaulieu E, et al. Expression of matrix metalloproteinases and their inhibitors in human brain tumors. Ann N Y Acad Sci 1999;886:236–239.
33. Wu L, Fan J, Matsumoto S, Watanabe T. Induction and regulation of matrix metalloproteinase-12 by cytokines and CD40 signaling in monocyte/macrophages. Biochem Biophys Res Commun 2000;269:808–815.
34. Xue M, Del Bigio MR. Acute tissue damage after injections of thrombin and plasmin into rat striatum. Stroke 2001;32: 2164–2169.

35. Johnston JB, Zhang K, Silva C, et al. HIV-1 Tat neurotoxicity is prevented by matrix metalloproteinase inhibitors. Ann Neurol 2001;49:230–241.
36. Anthony DC, Miller KM, Fearn S, et al. Matrix metalloproteinase expression in an experimentally-induced DTH model of multiple sclerosis in the rat CNS. J Neuroimmunol 1998;87: 62–72.
37. Yrjanheikki J, Tikka T, Keinanen R, et al. A tetracycline derivative, minocycline, reduces inflammation and protects against focal cerebral ischemia with a wide therapeutic window. Proc Natl Acad Sci USA 1999;96:13496–13500.
38. Popovic N, Schubart A, Goetz BD, et al. Inhibition of autoimmune encephalomyelitis by a tetracycline. Ann Neurol 2002; 51:215–223.
39. He Y, Appel S, Le W. Minocycline inhibits microglial activation and protects nigral cells after 6-hydroxydopamine injection into mouse striatum. Brain Res 2001;909:187–193.
40. Chen M, Ona VO, Li M, et al. Minocycline inhibits caspase-1 and caspase-3 expression and delays mortality in a transgenic mouse model of Huntington disease. Nat Med 2000;6: 797–801.
41. Lin S, Zhang Y, Dodel R, et al. Minocycline blocks nitric oxide-induced neurotoxicity by inhibition p38 MAP kinase in rat cerebellar granule neurons. Neurosci Lett 2001;315:61–64.
42. Zhu S, Stavrovskaya IG, Drozda M, et al. Minocycline inhibits cytochrome c release and delays progression of amyotrophic lateral sclerosis in mice. Nature 2002;417:74–78.
43. Corbett D, Nurse S. The problem of assessing effective neuroprotection in experimental cerebral ischemia. Prog Neurobiol 1998;54:531–548.
44. Seukeran DC, Eady EA, Cunliffe WJ. Benefit-risk assessment of acne therapies. Lancet 1997;349:1251–1252.
45. Shapiro LE, Knowles SR, Shear NH. Comparative safety of tetracycline, minocycline, and doxycycline. Arch Dermatol 1997; 133:1224–1230.
46. Sturkenboom MC, Meier CR, Jick H, Stricker BH. Minocycline and lupuslike syndrome in acne patients. Arch Intern Med 1999;159:493–497.
47. O'Dell JR. Is there a role for antibiotics in the treatment of patients with rheumatoid arthritis? Drugs 1999;57:279–282.
48. Wu DC, Jackson-Lewis V, Vila M, et al. Blockade of microglial activation is neuroprotective in the 1-methyl-4- phenyl-1,2,3,6-tetrahydropyridine mouse model of Parkinson disease. J Neurosci 2002;22:1763–1771.
49. Montaner J, Alvarez-Sabin J, Molina CA, et al. Matrix metalloproteinase expression is related to hemorrhagic transformation after cardioembolic stroke. Stroke 2001;32:2762–2767.
50. Sumii T, Lo EH. Involvement of matrix metalloproteinase in thrombolysis-associated hemorrhagic transformation after embolic focal ischemia in rats. Stroke 2002;33:831–836.
51. Castellanos M, Leira R, Serena J, et al. Plasma metalloproteinase-9 concentration predicts hemorrhagic transformation in acute ischemic stroke. Stroke 2003;34:40–46.